Hindawi Publishing Corporation
Abstract and Applied Analysis
Volume 2013, Article ID 483492, 18 pages
http://dx.doi.org/10.1155/2013/483492

Research Article

New Types of Nonlinear Waves and Bifurcation Phenomena in Schamel-Korteweg-de Vries Equation

Yun Wu[1,2] and Zhengrong Liu[1]

[1] *Department of Mathematics, South China University of Technology, Guangzhou, Guangdong 510640, China*
[2] *Department of Mathematics and Computer Science, Guizhou Normal University, Guiyang, Guizhou 550001, China*

Correspondence should be addressed to Zhengrong Liu; liuzhr@scut.edu.cn

Received 26 April 2013; Accepted 3 July 2013

Academic Editor: Chuanzhi Bai

We study the nonlinear waves described by Schamel-Korteweg-de Vries equation $u_t + (au^{1/2} + bu)u_x + \delta u_{xxx} = 0$. Two new types of nonlinear waves called compacton-like waves and kink-like waves are displayed. Furthermore, two kinds of new bifurcation phenomena are revealed. The first phenomenon is that the kink waves can be bifurcated from five types of nonlinear waves which are the bell-shape solitary waves, the blow-up waves, the valley-shape solitary waves, the kink-like waves, and the compacton-like waves. The second phenomenon is that the periodic-blow-up wave can be bifurcated from the smooth periodic wave.

1. Introduction and Preliminary

Consider the following Schamel-Korteweg-de Vries (S-KdV) equation [1, 2]:

$$u_t + \left(au^{1/2} + bu\right)u_x + \delta u_{xxx} = 0, \tag{1}$$

where a, b, and δ are constants.

Equation (1) arises in plasma physics in the study of ion acoustic solitons when electron trapping is present and also it governs the electrostatic potential for a certain electron distribution in velocity space. Tagare and Chakraborti [1] showed that (1) has solitary wave solution by applying direct integral method. Lee and Sakthivel [3] gave some exact traveling wave solutions of (1) by using exp-function method.

When $b = 0$, (1) becomes the Schamel equation [4]:

$$u_t + au^{1/2}u_x + \delta u_{xxx} = 0. \tag{2}$$

When $a = 0$, (1) becomes a well-known KdV equation

$$u_t + buu_x + \delta u_{xxx} = 0, \tag{3}$$

which has been studied successively by many authors (e.g., [5–8]).

The concept of compacton, soliton with compact support or strict localization of solitary waves, appeared in the work of Rosenau and Hyman [9] where a genuinely nonlinear dispersive equation $K(n;n)$ is defined by

$$u_t + a(u^n)_x + (u^n)_{xxx} = 0. \tag{4}$$

They found certain solitary wave solutions which vanish identically outside a finite core region. These solutions are called compactons.

Several studies have been conducted in [10–20]. The aim of these studies was to examine if other nonlinear dispersive equations may generate compactons structures.

In order to investigate the nonlinear waves of (1), letting $c > 0$ be wave speed and substituting $u = \varphi(\xi)$ with $\xi = x - ct$ into (1), it follows that

$$-c\varphi' + a\varphi^{1/2}\varphi' + b\varphi\varphi' + \delta\varphi''' = 0. \tag{5}$$

Integrating (5), we get

$$-c\varphi + \frac{2}{3}a\varphi^{3/2} + \frac{b}{2}\varphi^2 + \delta\varphi'' = 0. \tag{6}$$

Setting $\varphi' = y$ yields the following planar system:

$$\varphi' = y, \qquad y' = \frac{c}{\delta}\varphi - \frac{2a}{3\delta}\varphi^{3/2} - \frac{b}{2\delta}\varphi^2. \tag{7}$$

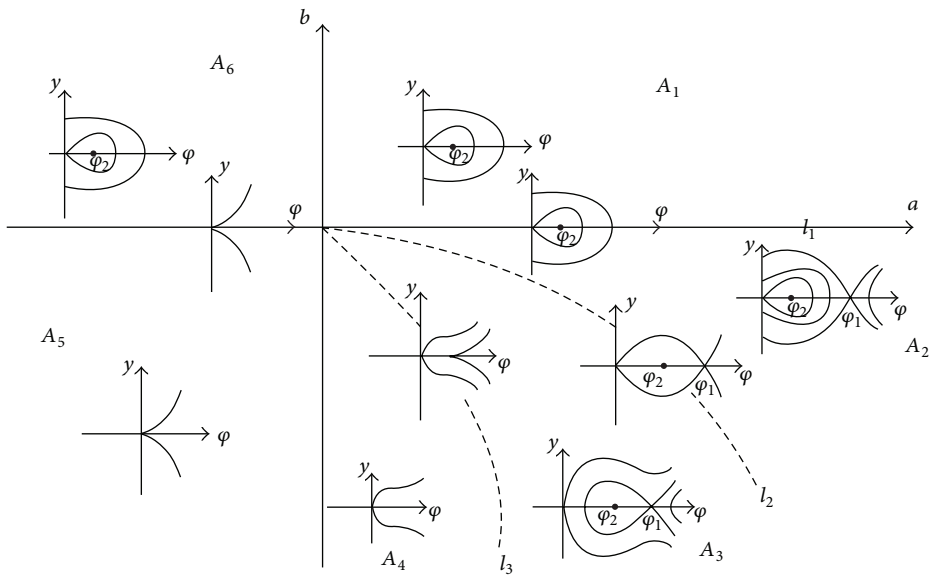

Figure 1: The bifurcation phase portraits of system (7) when $\delta > 0$.

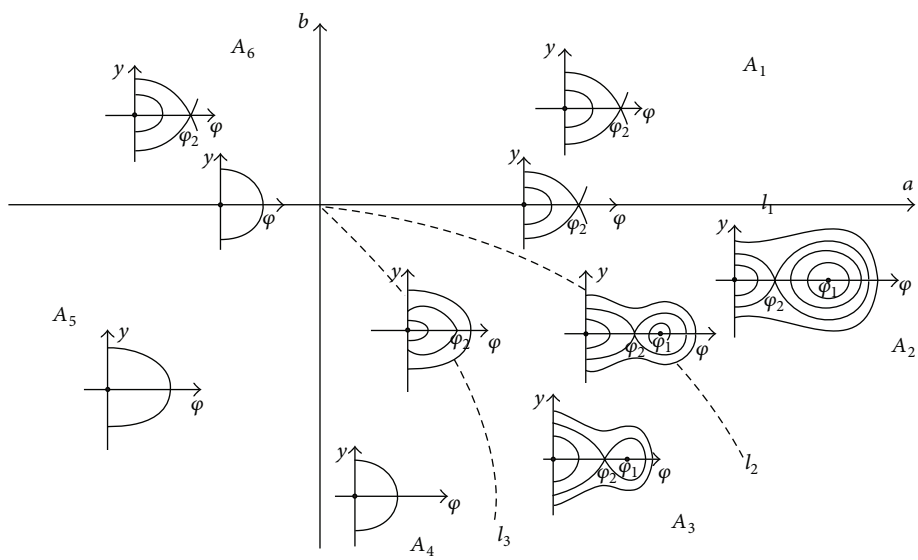

Figure 2: The bifurcation phase portraits of system (7) when $\delta < 0$.

Obviously, system (7) is a Hamiltonian system with Hamiltonian function

$$H(\varphi, y) = y^2 - \frac{c}{\delta}\varphi^2 + \frac{8a}{15\delta}\varphi^{5/2} + \frac{b}{3\delta}\varphi^3. \tag{8}$$

If one puts

$$f(\varphi) = \frac{c}{\delta}\varphi - \frac{2a}{3\delta}\varphi^{3/2} - \frac{b}{2\delta}\varphi^2, \qquad \Delta = 4a^2 + 18bc, \tag{9}$$

then one can see the following facts.

When $\Delta > 0$, $f(\varphi)$ has three zero points φ_0, φ_1, and φ_2 which possess expressions

$$\varphi_0 = 0, \qquad \varphi_1 = \left(\frac{-2a - \sqrt{\Delta}}{3b}\right)^2, \qquad \varphi_2 = \left(\frac{-2a + \sqrt{\Delta}}{3b}\right)^2. \tag{10}$$

When $\Delta = 0$, $f(\varphi)$ has two zero points φ_0 and φ^* which are denoted by

$$\varphi_0 = 0, \qquad \varphi^* = \frac{4a^2}{9b^2}. \tag{11}$$

When $\Delta < 0$, $f(\varphi)$ has one zero point $\varphi_0 = 0$.

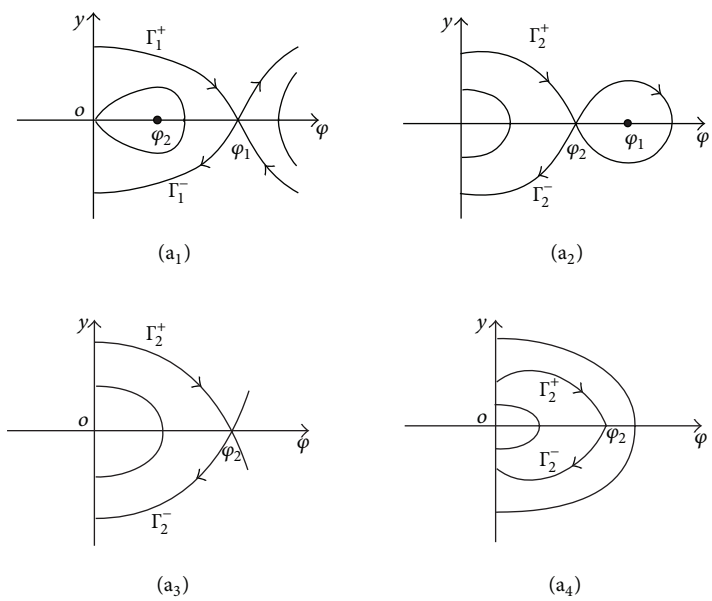

FIGURE 3: The graphs of orbits $\Gamma_1^{\pm}$ and $\Gamma_2^{\pm}$ when (a$_1$) $\delta > 0$ and $(a, b) \in A_2$, (a$_2$) $\delta < 0$ and $(a, b) \in A_2$ or A_3 or l_2, (a$_3$) $\delta < 0$ and $(a, b) \in A_1$ or A_6 or l_1 $(a > 0)$, and (a$_4$) $\delta < 0$ and $(a, b) \in l_3$.

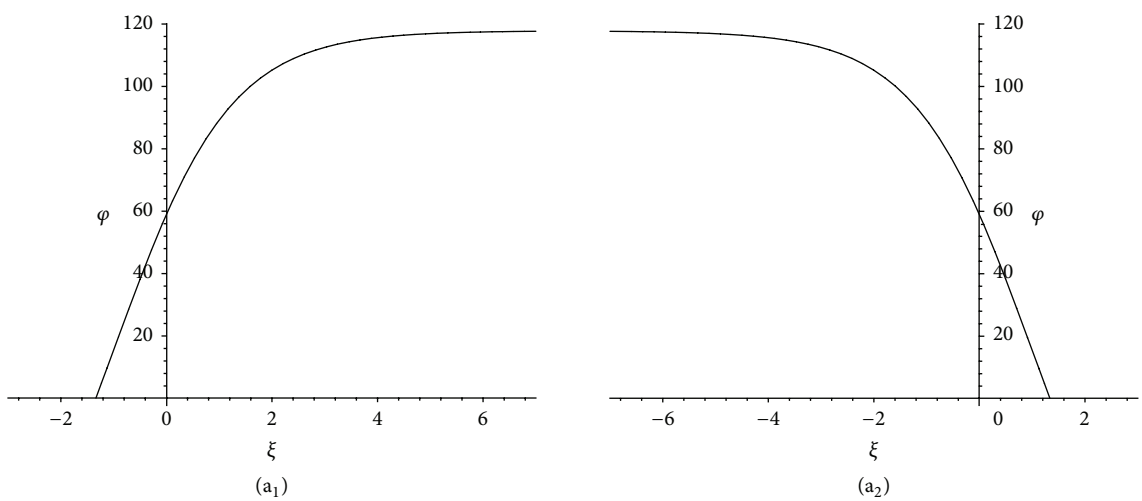

FIGURE 4: (Corresponding to Example 2). The simulation of integral curve of (6) when $a = 1/2$, $b = -2/45$, $c = 1$, and $\delta = 1$. (a$_1$) Initial conditions $\varphi(0) = 58.90576474$ and $\varphi'(0) = 38.27939786$. (a$_2$) Initial conditions $\varphi(0) = 58.90576474$ and $\varphi'(0) = -38.27939786$.

Letting $(\widetilde{\varphi}, 0)$ be one of the singular points of system (7), then the characteristic values at $(\widetilde{\varphi}, 0)$ are

$$\lambda = \pm\sqrt{f'(\widetilde{\varphi})}. \tag{12}$$

From the qualitative theory of dynamical systems, we get the following conclusions:

(1) if $f'(\widetilde{\varphi}) > 0$, then $(\widetilde{\varphi}, 0)$ is a saddle point,

(2) if $f'(\widetilde{\varphi}) < 0$, then $(\widetilde{\varphi}, 0)$ is a center point,

(3) if $f'(\widetilde{\varphi}) = 0$, then $(\widetilde{\varphi}, 0)$ is a degenerate saddle point.

On $a - b$ parametric plane, let l_1, l_2, and l_3, respectively, represent the following three curves:

$$\begin{aligned} l_1 &: b = 0, \\ l_2 &: b = -\frac{16a^2}{75c}, \\ l_3 &: b = -\frac{2a^2}{9c}. \end{aligned} \tag{13}$$

Let A_i $(i = 1, 2, \ldots, 6)$ represent the regions surrounded by l_1, l_2, l_3, and the coordinate axes (see Figures 1 and 2).

According to the previous analysis, we obtain the bifurcation phase portraits of system (7) as in Figures 1 and 2.

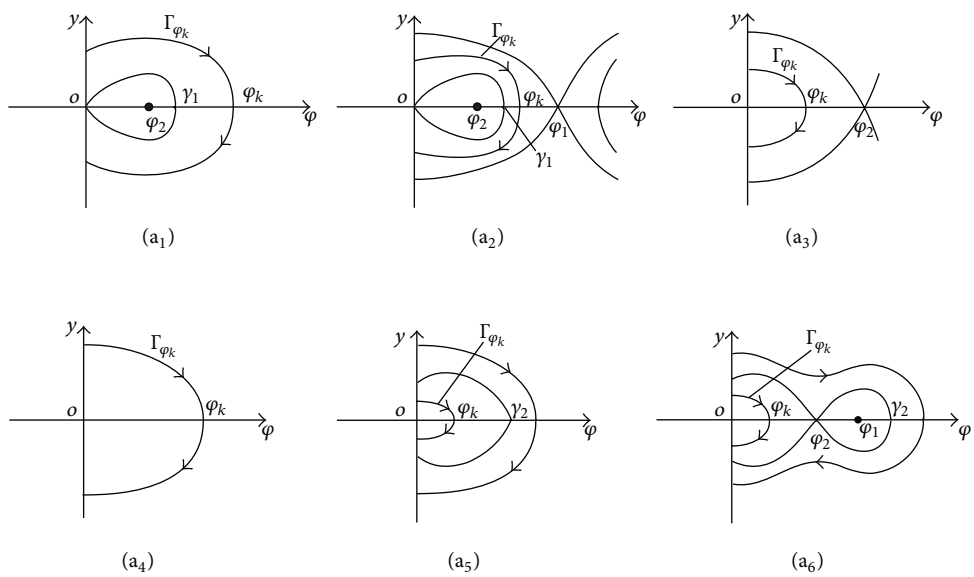

Figure 5: The graphs of orbit Γ_{φ_k} when (a$_1$) $\delta > 0$ and $(a, b) \in A_1$ or A_6 or l_1 $(a > 0)$, (a$_2$) $\delta > 0$ and $(a, b) \in A_2$, (a$_3$) $\delta < 0$ and $(a, b) \in A_1$ or A_6 or l_1 $(a > 0)$, (a$_4$) $\delta < 0$ and $(a, b) \in A_4$ or A_5 or l_1 $(a < 0)$, (a$_5$) $\delta < 0$ and $(a, b) \in l_3$, and (a$_6$) $\delta < 0$ and $(a, b) \in A_2$ or A_3 or l_2.

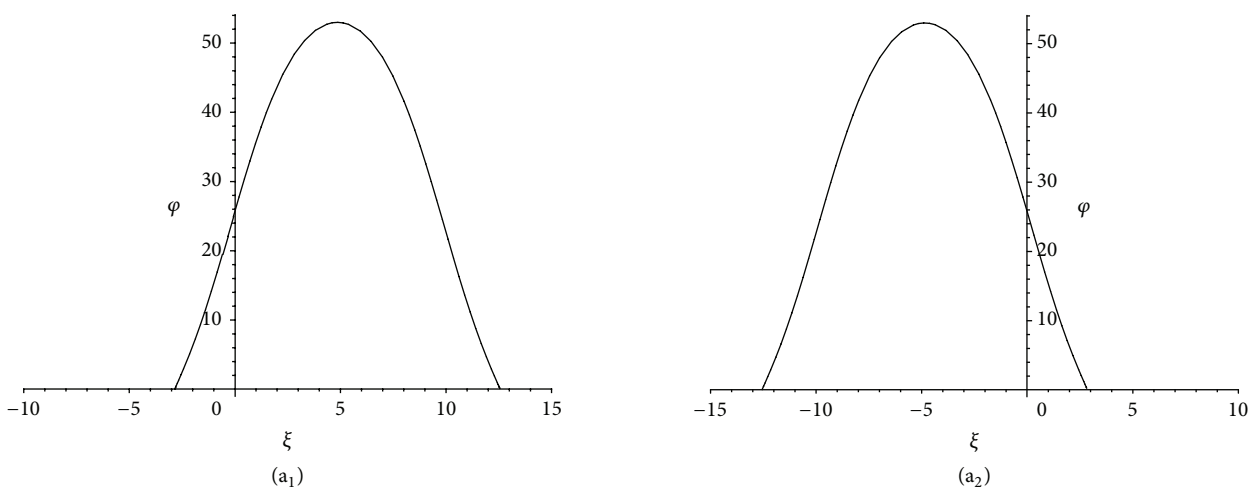

Figure 6: (Corresponding to Example 4). The simulation of integral curve of (6) when $a = 1$, $b = -157/3000$, $c = 1$, and $\delta = 1$. (a$_1$) Initial conditions $\varphi(0) = 26.49502557$ and $\varphi'(0) = 10.49025102$. (a$_2$) Initial conditions $\varphi(0) = 26.49502557$ and $\varphi'(0) = -10.49025102$.

In this paper, we study the nonlinear waves and their bifurcations in (1) by using the bifurcation method of dynamical systems [21–23]. We point out that there are two new types of nonlinear waves, kink-like waves and compacton-like waves [24–33]. Furthermore, we reveal two kinds of new bifurcation phenomena which are introduced in the abstract.

This paper is organized as follows. In Section 2, we display the two new types of nonlinear waves. We show the two kinds of new bifurcation phenomena in Sections 3 and 4. A brief conclusion is given in Section 5.

2. Two New Types of Nonlinear Waves

In this section, we display two new types of nonlinear waves defined by (1).

2.1. Kink-Like Waves

Proposition 1. *(1) When the parameters satisfy $\delta > 0$, $a > 0$, and $-16a^2/75c < b < 0$, (1) has a kink-like wave solution $u_a^+ = \varphi(\xi)$ and an antikink-like wave solution $u_a^- = \varphi(\xi)$, respectively, which are hidden in the following equations:*

$$\int_{\varphi_1/2}^{\varphi} \frac{ds}{\sqrt{(c/\delta)\, s^2 - (8a/15\delta)\, s^{5/2} - (b/3\delta)\, s^3 + h_1}} = \xi, \quad \xi \in \left(-\xi_1^0, \infty\right), \tag{14}$$

$$\int_{\varphi_1/2}^{\varphi} \frac{ds}{\sqrt{(c/\delta)\, s^2 - (8a/15\delta)\, s^{5/2} - (b/3\delta)\, s^3 + h_1}} = -\xi, \quad \xi \in \left(-\infty, \xi_1^0\right), \tag{15}$$

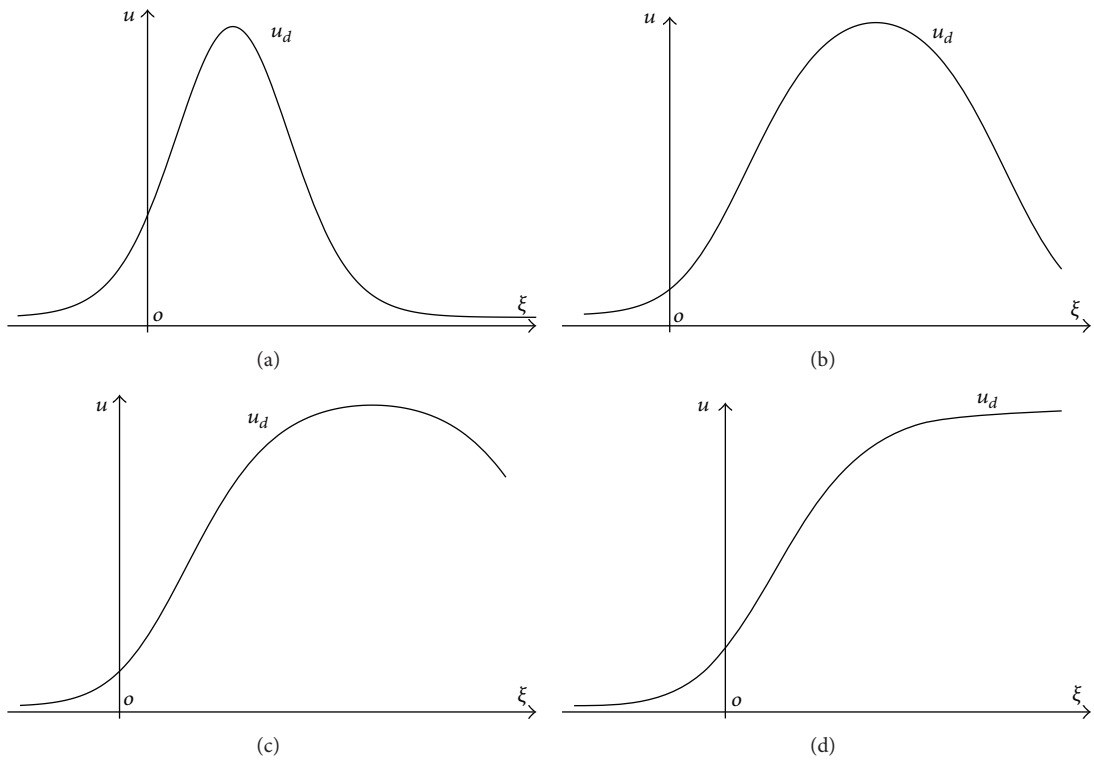

Figure 7: (The kink wave is bifurcated from the bell-shape solitary wave). The varying process for the graph of u_d when $c > 0$, $\delta > 0$, $a > 0$, $\lambda > 0$ and $b \to -16a^2/75c + 0$. Where $c = 1$, $\delta = 1$, $a = 1$, $\lambda = 50$ and (a) $b = -16a^2/75c + 10^{-1}$. (b) $b = -16a^2/75c + 10^{-3}$. (c) $b = -16a^2/75c + 10^{-4}$. (d) $b = -16a^2/75c + 10^{-7}$.

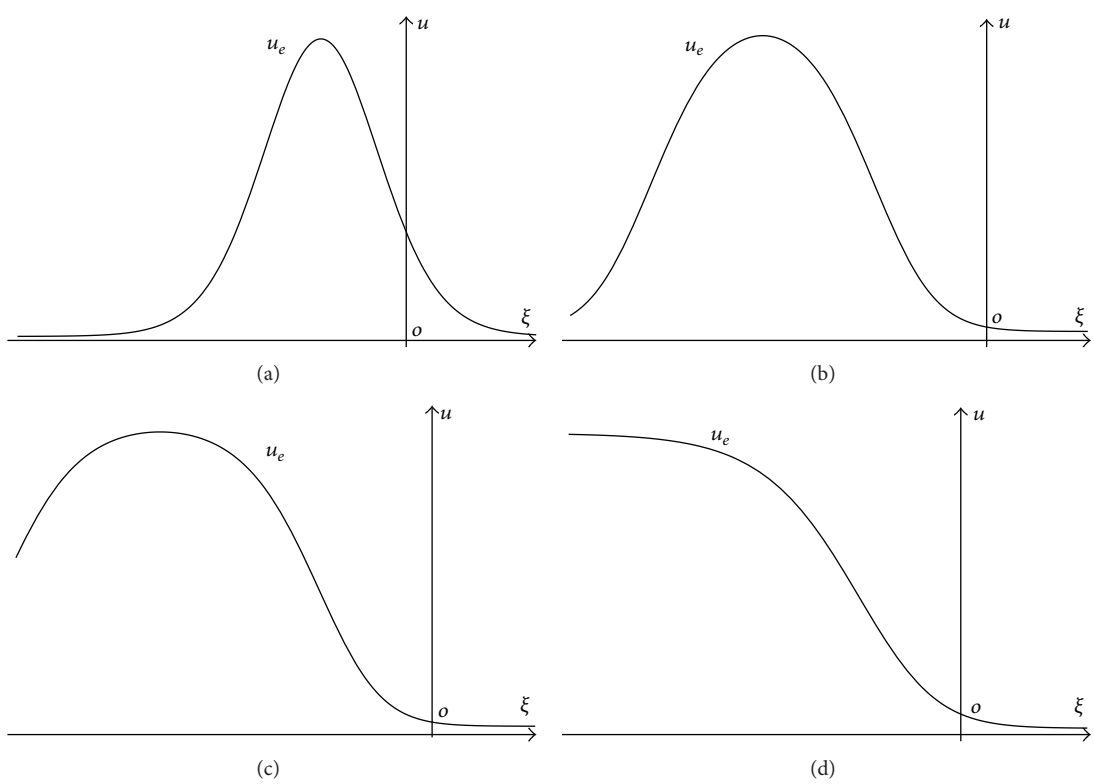

Figure 8: (The anti-kink wave is bifurcated from the bell-shape solitary wave). The varying process for the graph of u_e when $c > 0$, $\delta > 0$, $a > 0$, $\lambda > 0$ and $b \to -16a^2/75c + 0$. Where $c = 1$, $\delta = 1$, $a = 1$, $\lambda = 50$ and (a) $b = -16a^2/75c + 10^{-1}$. (b) $b = -16a^2/75c + 10^{-3}$. (c) $b = -16a^2/75c + 10^{-4}$. (d) $b = -16a^2/75c + 10^{-7}$.

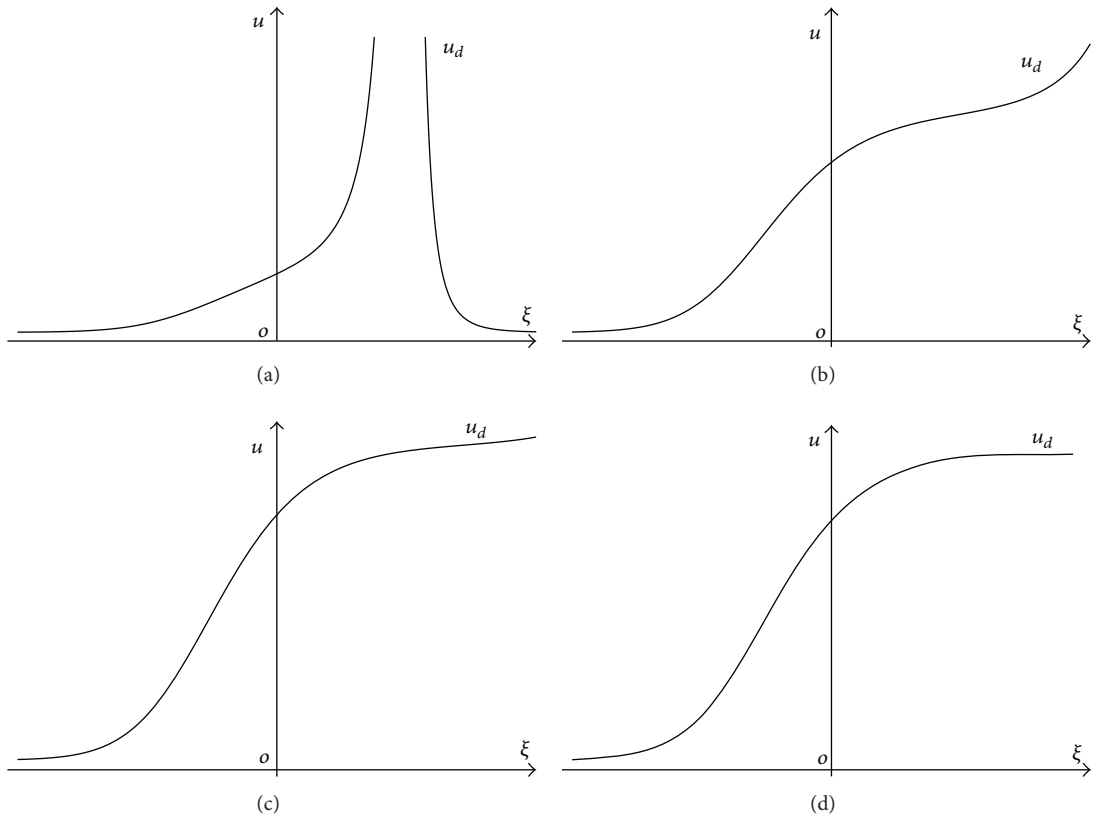

Figure 9: (The kink wave is bifurcated from the blow-up wave). The varying process for the graph of u_d when $c > 0$, $\delta > 0$, $a > 0$, $\lambda > 0$, and $b \to -16a^2/75c - 0$, where $c = 1$, $\delta = 1$, $a = 1$, $\lambda = 1$, and (a) $b = -16a^2/75c - 10^{-2}$. (b) $b = -16a^2/75c - 10^{-4}$. (c) $b = -16a^2/75c - 10^{-5}$. (d) $b = -16a^2/75c - 10^{-9}$.

where

$$\xi_1^0 = \int_0^{\varphi_1/2} \frac{ds}{\sqrt{(c/\delta)\, s^2 - (8a/15\delta)\, s^{5/2} - (b/3\delta)\, s^3 + h_1}} \quad (16)$$

and $h_1 = H(\varphi_1, 0)$.

(2) When the parameters satisfy one of the following Cases.

Case 1. $\delta < 0$, $a > 0$, *and* $-2a^2/9c < b < 0$,

Case 2. $\delta < 0$, *and* $b > 0$,

Case 3. $\delta < 0$, $a > 0$, *and* $b = 0$,

Case 4. $\delta < 0$, $a > 0$, *and* $b = -2a^2/9c$.

Equation (1) *has a kink-like wave solution* $u_b^+ = \varphi(\xi)$ *and an antikink-like wave solution* $u_b^- = \varphi(\xi)$, *respectively, which are hidden in the following equations:*

$$\begin{aligned} &\int_{\varphi_2/2}^{\varphi} \frac{ds}{\sqrt{(c/\delta)\, s^2 - (8a/15\delta)\, s^{5/2} - (b/3\delta)\, s^3 + h_2}} = \xi, \\ &\qquad \xi \in \left(-\xi_2^0, \infty\right), \\ &\int_{\varphi_2/2}^{\varphi} \frac{ds}{\sqrt{(c/\delta)\, s^2 - (8a/15\delta)\, s^{5/2} - (b/3\delta)\, s^3 + h_2}} = -\xi, \\ &\qquad \xi \in \left(-\infty, \xi_2^0\right), \end{aligned} \quad (17)$$

where

$$\xi_2^0 = \int_0^{\varphi_2/2} \frac{ds}{\sqrt{(c/\delta)\, s^2 - (8a/15\delta)\, s^{5/2} - (b/3\delta)\, s^3 + h_2}} \quad (18)$$

and $h_2 = H(\varphi_2, 0)$.

Proof. (1) Under the condition $\delta > 0$, $a > 0$, and $-16a^2/75c < b < 0$, $(\varphi_1, 0)$ is a saddle point and on its left side there are two orbits $\Gamma_1^{\pm}$ connecting with it (see Figure 3(a_1)).

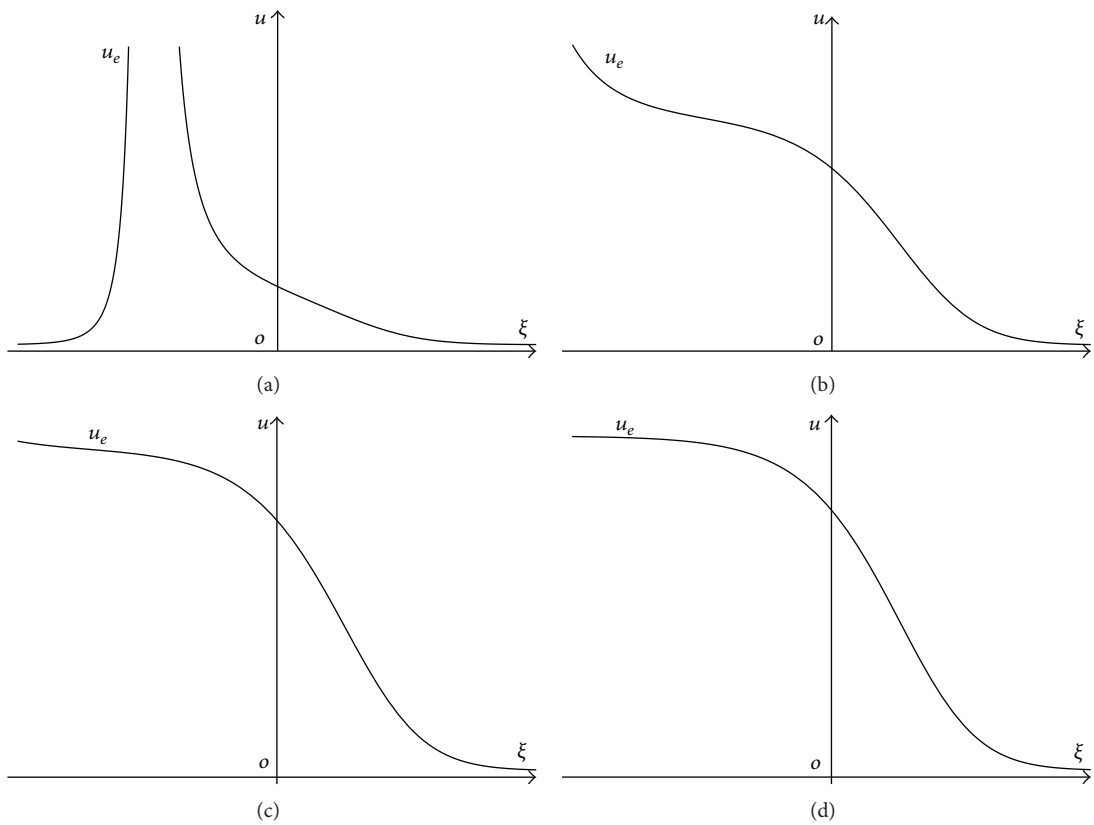

Figure 10: (The antikink wave is bifurcated from the blow-up wave). The varying process for the graph of u_e when $c > 0$, $\delta > 0$, $a > 0$, $\lambda > 0$, and $b \to -16a^2/75c - 0$, where $c = 1$, $\delta = 1$, $a = 1$, $\lambda = 1$, and (a) $b = -16a^2/75c - 10^{-2}$. (b) $b = -16a^2/75c - 10^{-4}$. (c) $b = -16a^2/75c - 10^{-5}$. (d) $b = -16a^2/75c - 10^{-9}$.

In (8), letting $h_1 = H(\varphi_1, 0)$, it follows that

$$\Gamma_1^{\pm} : y = \pm\sqrt{\frac{c}{\delta}\varphi^2 - \frac{8a}{15\delta}\varphi^{5/2} - \frac{b}{3\delta}\varphi^3 + h_1} \quad (0 < \varphi < \varphi_1). \tag{19}$$

On $\Gamma_1^{\pm}$ suppose $\varphi(0) = \varphi_1/2$. Substituting (19) into (7) and integrating them along Γ_1^+ and Γ_1^-, respectively, we get (14)–(16).

(2) Under one of Cases 1–4, $(\varphi_2, 0)$ is a saddle point and on its left side there are two orbits $\Gamma_2^{\pm}$ connecting with it (see Figures 3(a_2)–3(a_4)).

In (8), letting $h_2 = H(\varphi_2, 0)$, it follows that

$$\Gamma_2^{\pm} : y = \pm\sqrt{\frac{c}{\delta}\varphi^2 - \frac{8a}{15\delta}\varphi^{5/2} - \frac{b}{3\delta}\varphi^3 + h_2} \quad (0 < \varphi < \varphi_2). \tag{20}$$

Similar to the proof of (1), we get the results of (2). □

Next, we simulate the planar graphs of the kink-like waves for those data given in Example 2.

Example 2 (Corresponding to Proposition 1 (1)). Giving $a = 1/2$, $b = -2/45$, $c = 1$, and $\delta = 1$, we get $\varphi_1 = 117.81152949$ and $\varphi(0) = \varphi_1/2 = 58.90576474$. Note that orbits $\Gamma_1^{\pm}$ have expressions (19). From (19) we get $y_1^+(0) = 38.27939786$ and $y_1^-(0) = -38.27939786$. These imply that Γ_1^+ passes point $(\varphi(0), y_1^+(0))$ and Γ_1^- passes point $(\varphi(0), y_1^-(0))$. Thus letting $\varphi(0) = \varphi_1/2$ and $\varphi'(0) = y_1^+(0)$ as the initial conditions of (6), we get the simulation of the integral curve which corresponds to Γ_1^+ as Figure 4(a_1). Meanwhile, choosing $\varphi(0) = \varphi_1/2$ and $\varphi'(0) = y_1^-(0)$ as the initial conditions of (6), we get the simulation of the integral curve which corresponds to Γ_1^- as in Figure 4(a_2).

2.2. Compacton-Like Waves

Proposition 3. *Let φ_k be an initial value when parameters and initial value satisfy one of the following Cases.*

Case 1. $\delta > 0$, $b > 0$, *and* $\varphi_k > \gamma_1$,

Case 2. $\delta > 0$, $a > 0$, $b = 0$, *and* $\varphi_k > \gamma_1$,

Case 3. $\delta > 0$, $a > 0$, $-16a^2/75c < b < 0$, *and* $\gamma_1 < \varphi_k < \varphi_1$,

Case 4. $\delta < 0$, $b > 0$, *and* $0 < \varphi_k < \varphi_2$,

Case 5. $\delta < 0$, $a > 0$, $b = 0$, *and* $0 < \varphi_k < \varphi_2$,

Case 6. $\delta < 0$, $a < 0$, $b \le 0$, *and* $\varphi_k > 0$,

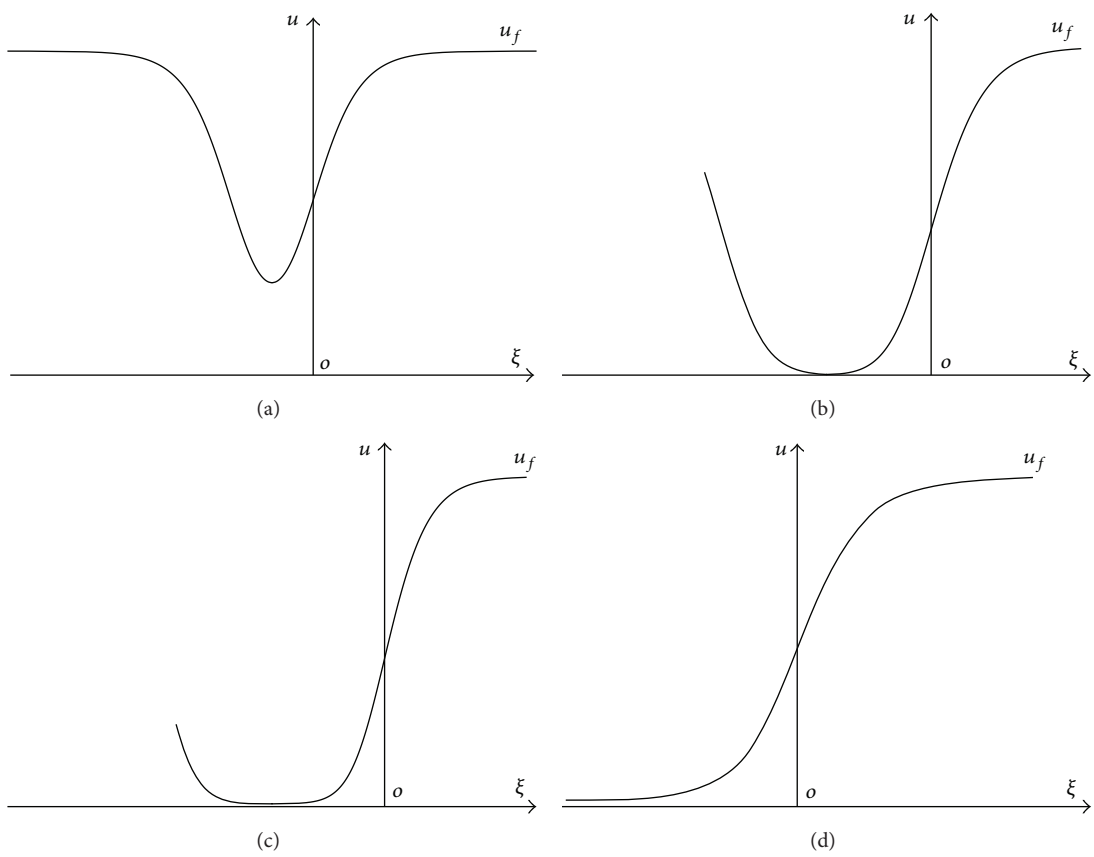

Figure 11: (The kink wave is bifurcated from the valley-shape solitary wave). The varying process for the graph of u_f when $c > 0, \delta > 0, a > 0$, and $b \to -16a^2/75c - 0$, where $c = 1$, $\delta = 1$, $a = 1/2$, and (a) $b = -16a^2/75c - 10^{-3}$. (b) $b = -16a^2/75c - 10^{-7}$. (c) $b = -16a^2/75c - 10^{-8}$. (d) $b = -16a^2/75c - 10^{-10}$.

Case 7. $\delta < 0$, $a > 0$, $b < -2a^2/9c$, *and* $\varphi_k > 0$,

Case 8. $\delta < 0$, $a > 0$, $b = -2a^2/9c$, *and* $\varphi_k \neq \gamma_2 (= \varphi_2)$,

Case 9. $\delta < 0$, $a > 0$, $-2a^2/9c < b < 0$, *and* $\varphi_k > \gamma_2$ *or* $0 < \varphi_k < \varphi_2$.

Equation (1) *has compacton-like wave solutions* $u_c^+ = \varphi(\xi)$ *and* $u_c^- = \varphi(\xi)$, *respectively, which are hidden in the following equations:*

$$\int_{\varphi_k/2}^{\varphi} \frac{ds}{\sqrt{(c/\delta)\, s^2 - (8a/15\delta)\, s^{5/2} - (b/3\delta)\, s^3 + h_{\varphi_k}}} = \xi, \qquad \xi \in \left(-\xi_3^0, \xi_4^0\right),$$
$$\int_{\varphi_k/2}^{\varphi} \frac{ds}{\sqrt{(c/\delta)\, s^2 - (8a/15\delta)\, s^{5/2} - (b/3\delta)\, s^3 + h_{\varphi_k}}} = -\xi, \qquad \xi \in \left(-\xi_4^0, \xi_3^0\right), \tag{21}$$

where

$$\xi_3^0 = \int_0^{\varphi_k/2} \frac{ds}{\sqrt{(c/\delta)\, s^2 - (8a/15\delta)\, s^{5/2} - (b/3\delta)\, s^3 + h_{\varphi_k}}}, \tag{22}$$

$$\xi_4^0 = 2\int_{\varphi_k/2}^{\varphi_k} \frac{ds}{\sqrt{(c/\delta)\, s^2 - (8a/15\delta)\, s^{5/2} - (b/3\delta)\, s^3 + h_{\varphi_k}}} + \xi_3^0, \tag{23}$$

and $h_{\varphi_k} = H(\varphi_k, 0)$.

Proof. Under one of Cases 1–9, there is an orbit Γ_{φ_k} passing point $(\varphi_k, 0)$ (see Figure 5 (a_1)–5(a_6)).

In (8), letting $h_{\varphi_k} = H(\varphi_k, 0)$, it follows that

$$\Gamma_{\varphi_k} : y^2 = \frac{c}{\delta}\varphi^2 - \frac{8a}{15\delta}\varphi^{5/2} - \frac{b}{3\delta}\varphi^3 + h_{\varphi_k} \quad (0 < \varphi < \varphi_k). \tag{24}$$

On Γ_{φ_k} suppose $\varphi(0) = \varphi_k/2$. Substituting (24) into (7) and integrating it along Γ_{φ_k}, respectively, we obtain (21)–(23). □

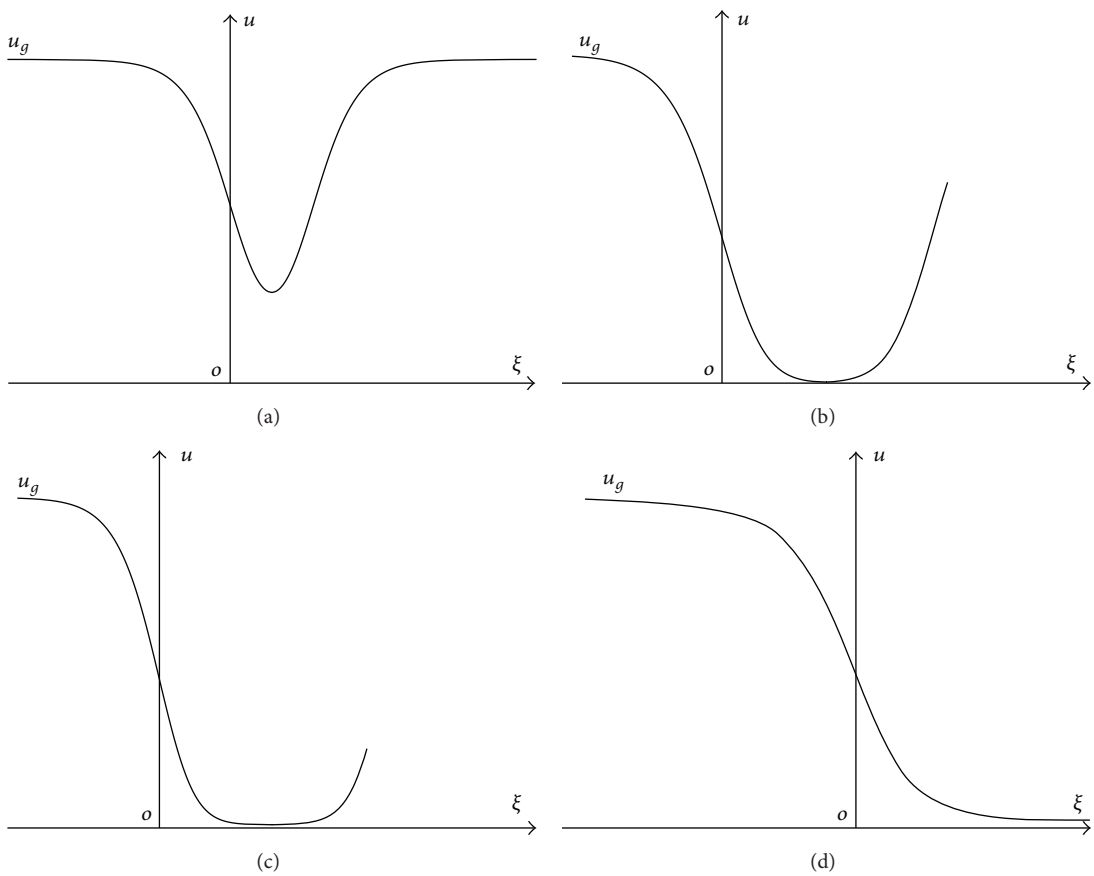

Figure 12: (The antikink wave is bifurcated from the valley-shape solitary wave). The varying process for the graph of u_g when $c > 0$, $\delta > 0$, $a > 0$, and $b \to -16a^2/75c - 0$, where $c = 1$, $\delta = 1$, $a = 1/2$, and (a) $b = -16a^2/75c - 10^{-3}$. (b) $b = -16a^2/75c - 10^{-7}$. (c) $b = -16a^2/75c - 10^{-8}$. (d) $b = -16a^2/75c - 10^{-10}$.

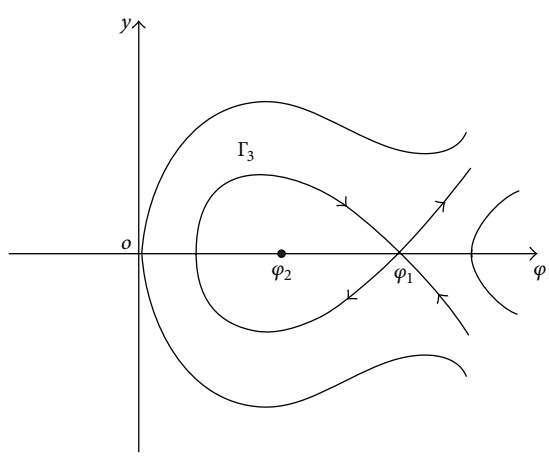

Figure 13: The graph of orbit Γ_3 when $\delta > 0$ and $(a, b) \in A_3$.

Next, we simulate the planar graphs of the compacton-like waves for those data given in Example 4.

Example 4 (Corresponding to Proposition 3 Case (3)). Giving $a = 1/2$, $b = -157/3000$, $c = 1$, and $\delta = 1$, we get $\varphi_1 = 62.46353941$ and $\gamma_1 = 43.51656288$. Note that orbit Γ_{φ_k} has expression (24). Letting $\varphi_k = (\varphi_1 + \gamma_1)/2$, it follows that $\varphi(0) = 26.49502557$. From (24) we get $y(0) = \pm 10.49025102$. Thus letting $\varphi(0) = 26.49502557$ and $\varphi'(0) = 10.49025102$ as the initial conditions of (6), we get the simulation of

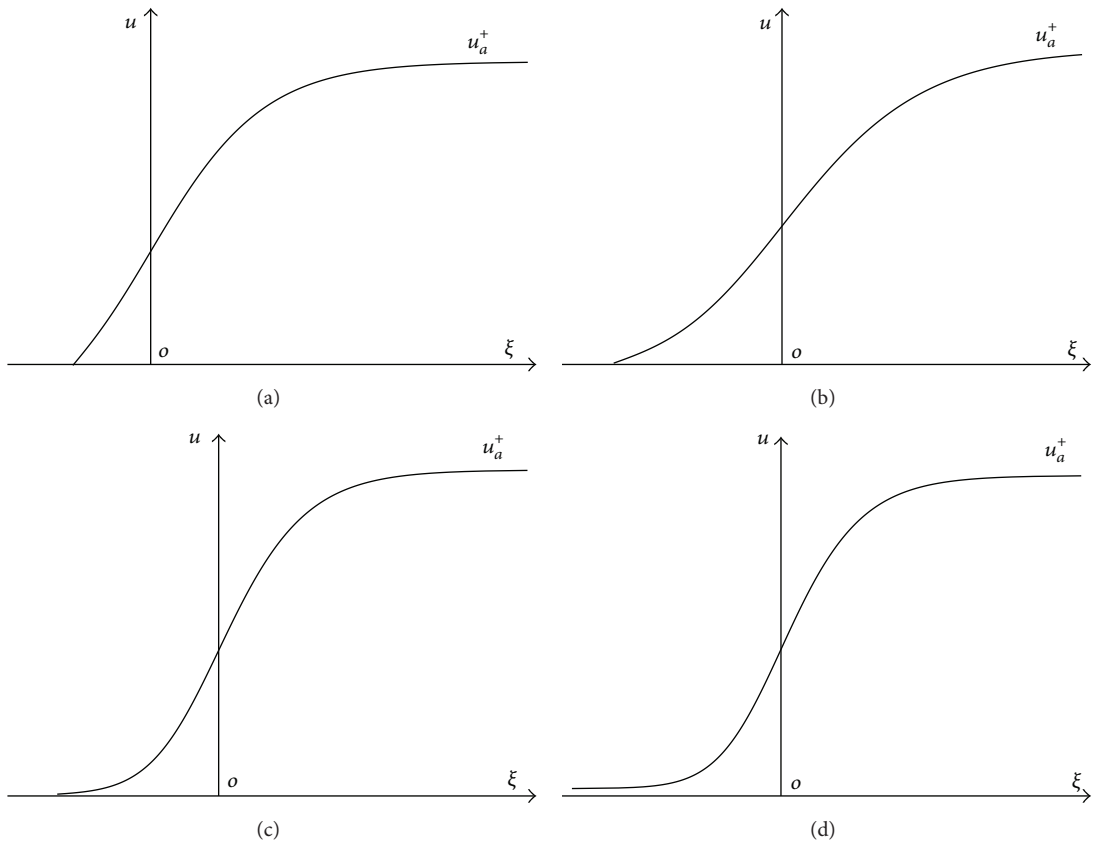

Figure 14: (The kink wave is bifurcated from the kink-like wave). The varying process for the graph of u_a^+ when $c > 0$, $\delta > 0$, $a > 0$, and $b \to -16a^2/75c + 0$, where $c = 1$, $\delta = 1$, $a = 1/2$, and (a) $b = -16a^2/75c + 10^{-3}$. (b) $b = -16a^2/75c + 10^{-4}$. (c) $b = -16a^2/75c + 10^{-6}$. (d) $b = -16a^2/75c + 10^{-8}$.

the integral curve as in Figure 6(a_1). Meanwhile, choosing $\varphi(0) = 26.49502557$ and $\varphi'(0) = -10.49025102$ as the initial conditions of (6), we get the simulation of the integral curve as Figure 6(a_2).

3. Bifurcation of the Kink Waves

In this section, we show that the kink waves can be bifurcated from five other waves.

3.1. Bifurcation from Bell-Shape Solitary Waves

Proposition 5. *For $ab \neq 0$ and $\delta > 0$, (1) has two nonlinear wave solutions*

$$u_d = \left(\frac{4\alpha\lambda}{\lambda^2 e^{-\tau_1\xi} - 2\lambda\beta + (\beta^2 - 4\alpha)\, e^{\tau_1\xi}}\right)^2,$$
$$u_e = \left(\frac{4\alpha\lambda}{\lambda^2 e^{\tau_1\xi} - 2\lambda\beta + (\beta^2 - 4\alpha)\, e^{-\tau_1\xi}}\right)^2, \tag{25}$$

where

$$\alpha = pq, \qquad \beta = -(p+q), \qquad \tau_1 = \frac{1}{2}\sqrt{\frac{c}{\delta}}, \tag{26}$$

$$p = \sqrt{\gamma_1} = \frac{-4a + \sqrt{16a^2 + 75bc}}{5b}, \tag{27}$$

$$q = \frac{-4a - \sqrt{16a^2 + 75bc}}{5b}, \tag{28}$$

and $\lambda \neq 0$ is an arbitrary real number. These solutions possess the following properties.

(1) *If $\lambda > 0$, $a > 0$, and $b = -16a^2/75c$, then u_d and u_e become*

$$u_d^* = \left(\frac{4\alpha}{\lambda e^{-\tau_1\xi} - 2\beta}\right)^2,$$
$$u_e^* = \left(\frac{4\alpha}{\lambda e^{\tau_1\xi} - 2\beta}\right)^2, \tag{29}$$

which represent a kink wave and an antikink wave.

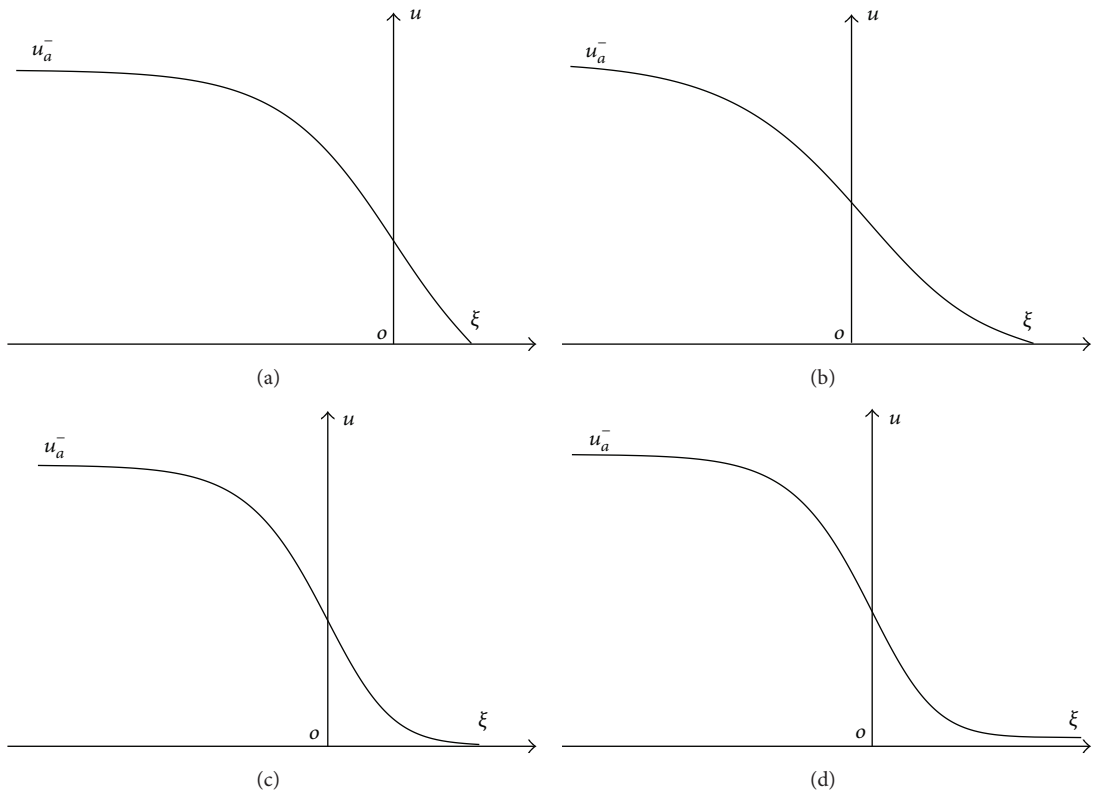

Figure 15: (The antikink wave is bifurcated from the antikink-like wave). The varying process for the graph of u_a^- when $c > 0$, $\delta > 0$, $a > 0$, and $b \to -16a^2/75c + 0$, where $c = 1$, $\delta = 1$, $a = 1/2$, and (a) $b = -16a^2/75c + 10^{-3}$. (b) $b = -16a^2/75c + 10^{-4}$. (c) $b = -16a^2/75c + 10^{-6}$. (d) $b = -16a^2/75c + 10^{-8}$.

In particular, when $\alpha = pq = -3c/b$, $\beta = -(p+q) = 8a/5b$, $c = -16a^2/75b$, $\lambda = a_0$, and $\xi = x - ct$, u_d^* and u_e^* become

$$u_1 = \frac{16a_0^2a^2}{\left(4a\exp\left(\pm(2/5)\sqrt{-1/3b\delta}a\left(x+\left(16a^2/75b\right)t\right)\right)-5a_0b\right)^2}, \tag{30}$$

which was given by Lee and Sakthivel [3]. This implies that u_1 is the special case of u_d or u_e.

(2) *If $\lambda = \sqrt{\beta^2 - 4\alpha}$, then $u_d = u_e$ and become*

$$u_{de}^* = \left(\frac{2\alpha}{\sqrt{\beta^2 - 4\alpha}\cosh(\tau_1\xi) - \beta}\right)^2. \tag{31}$$

When (a, b) belongs to one of the regions A_2, A_6, u_{de}^* represents a hyperbolic solitary wave.

In particular, when $\alpha = pq = -3c/b$, and $\beta = -(p + q) = 8a/5b$, u_{de}^* becomes

$$u_2 = \left(\frac{15c}{4a + \sqrt{16a^2 + 75bc}\cosh\left((1/2)\sqrt{c/\delta}\xi\right)}\right)^2, \tag{32}$$

which was obtained by Tagare and Chakraborti [3]. This implies that u_2 is the special case of u_d or u_e.

(3) *Under one of the following Cases.*

Case 1. $\lambda > 0$, $\lambda \neq \sqrt{\beta^2 - 4\alpha}$, and (a, b) belongs to one of the regions A_2, A_6,

Case 2. $\lambda < 0$, $\lambda \neq -\sqrt{\beta^2 - 4\alpha}$, and $(a, b) \in A_1$, $u_d \neq u_e$ and they represent two bell-shape solitary waves.

In particular, when $(a, b) \in A_2$ in Case 1 and $b \to 0 - 0$, u_d and u_e become

$$u_d^\circ = \frac{225c^2}{4a^2\left(1 + e^{-\tau_1\xi}\right)^4}, \tag{33}$$

$$u_e^\circ = \frac{225c^2}{4a^2\left(1 + e^{\tau_1\xi}\right)^4}, \tag{34}$$

which are the solutions of the Schamel equation.

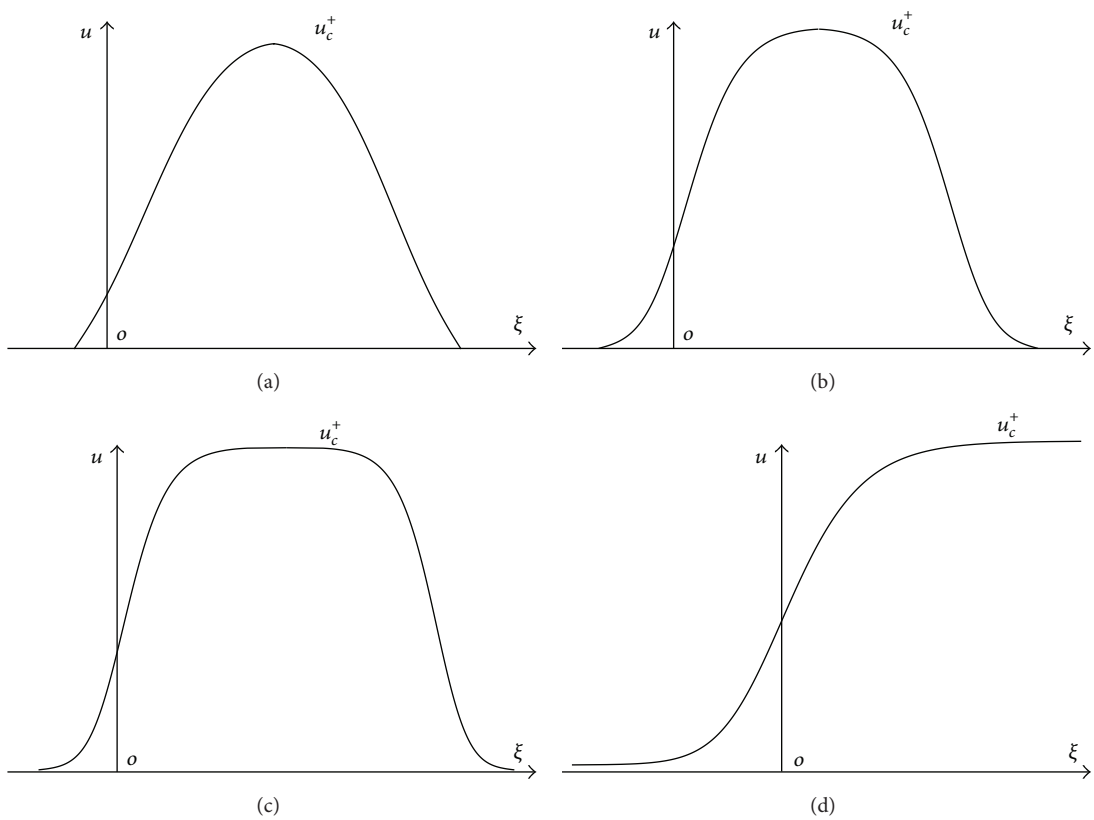

Figure 16: (The kink wave is bifurcated from the compacton-like wave). The varying process for the graph of u_c^+ when $c > 0$, $\delta > 0$, $a > 0$, and $b \to -16a^2/75c + 0$, where $c = 1$, $\delta = 1$, $a = 1/2$, and (a) $b = -16a^2/75c + 10^{-3}$. (b) $b = -16a^2/75c + 10^{-4}$. (c) $b = -16a^2/75c + 10^{-6}$. (d) $b = -16a^2/75c + 10^{-8}$.

When $(a, b) \in A_2$ in Case 1 and $b \to -16a^2/75c + 0$, the two bell-shape solitary waves u_d and u_e become a kink wave and an antikink wave with the expressions (29). *For the varying process, see Figures 7 and 8.*

Proof. In (8), letting $h_0 = H(0, 0)$, it follows that

$$y = \pm\sqrt{\frac{c}{\delta}\varphi^2 - \frac{8a}{15\delta}\varphi^{5/2} - \frac{b}{3\delta}\varphi^3}. \tag{35}$$

Substituting (35) into $\mathrm{d}\varphi/\mathrm{d}\xi = y$, we have

$$\frac{d\varphi}{d\xi} = \pm\sqrt{\frac{c}{\delta}\varphi^2 - \frac{8a}{15\delta}\varphi^{5/2} - \frac{b}{3\delta}\varphi^3}. \tag{36}$$

Let $\varphi = w^2$, (36) becomes

$$\frac{2w\mathrm{d}w}{d\xi} = \pm\sqrt{\frac{c}{\delta}w^4 - \frac{8a}{15\delta}w^5 - \frac{b}{3\delta}w^6}. \tag{37}$$

Integrating (37), we have

$$\int_{\nu}^{w} \frac{ds}{s\sqrt{c/\delta - (8a/15\delta)\,s - (b/3\delta)\,s^2}} = \pm\frac{1}{2}\xi, \tag{38}$$

where ν is an arbitrary constant.

Completing the previous integral and solving the equation for φ, it follows that

$$\varphi = \left(\frac{4\alpha\lambda e^{\mp\tau_1\xi}}{\lambda^2 e^{\mp 2\tau_1\xi} - 2\lambda\beta e^{\mp\tau_1\xi} + (\beta^2 - 4\alpha)}\right)^2, \tag{39}$$

where $\lambda = \lambda(\nu)$ is an arbitrary real number. From (39) we obtain the solutions u_d and u_e as (25).

In (25) letting $b = -16a^2/75c$, we get (29). From (25) and (29), we get the result (1) of Proposition 5.

When $\lambda = \sqrt{\beta^2 - 4\alpha}$, via (25) it follows that

$$\begin{aligned} u_d &= u_e \\ &= \left(\frac{4\alpha}{\lambda\left(e^{-\tau_1\xi} + e^{\tau_1\xi}\right) - 2\beta}\right)^2 \\ &= \left(\frac{2\alpha}{\lambda\cosh\tau_1\xi - \beta}\right)^2 \\ &= u_{de}^* \end{aligned} \tag{40}$$

(see (31)).

Thus, we get the result (2) of Proposition 5.

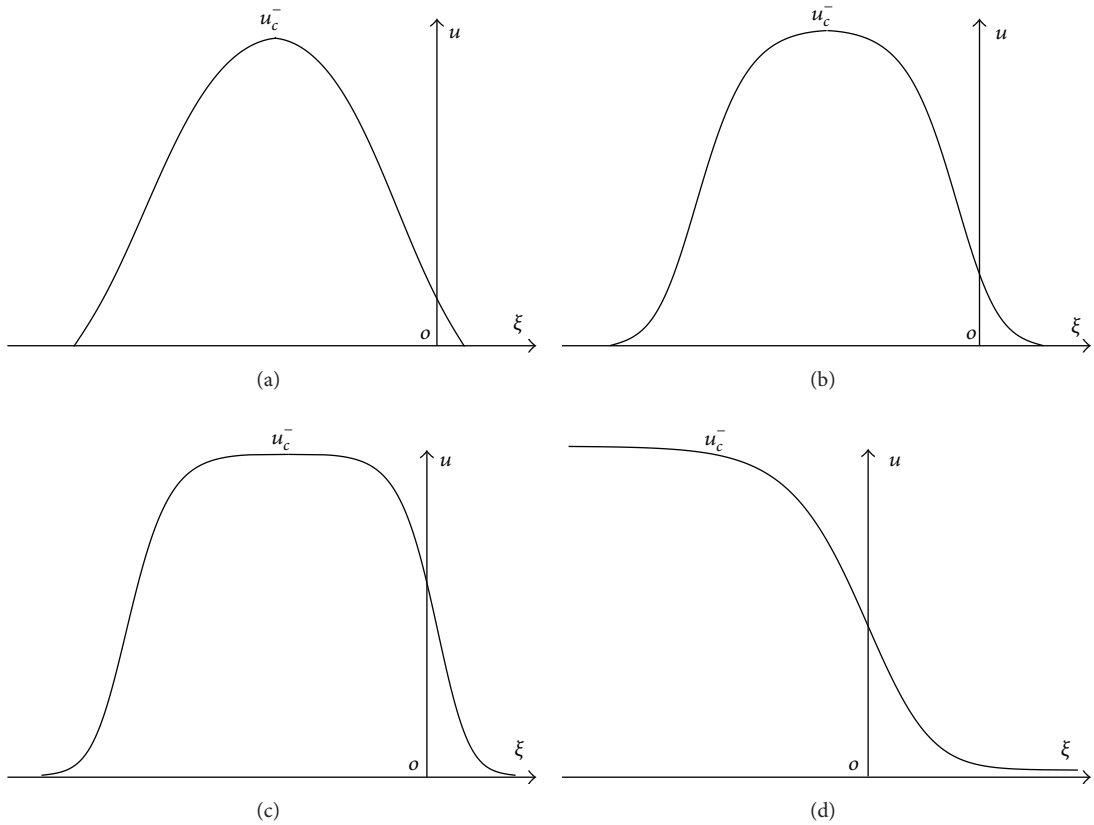

Figure 17: (The antikink wave is bifurcated from the compacton-like wave). The varying process for the graph of u_c^- when $c > 0$, $\delta > 0$, $a > 0$, and $b \to -16a^2/75c + 0$, where $c = 1$, $\delta = 1$, $a = 1/2$, and (a) $b = -16a^2/75c + 10^{-3}$. (b) $b = -16a^2/75c + 10^{-4}$. (c) $b = -16a^2/75c + 10^{-6}$. (d) $b = -16a^2/75c + 10^{-8}$.

In (38), letting $\nu = p$ (see (27)), it follows that

$$\begin{aligned}\lambda &= \frac{\beta p + 2\alpha}{p} \\ &= -\frac{2\sqrt{16a^2 + 75bc}}{5b}.\end{aligned} \tag{41}$$

Letting $b \to 0 - 0$, then

$$\begin{aligned}\lim_{b\to 0-0} \frac{\alpha}{\lambda} &= \lim_{b\to 0-0} \frac{3c}{b} \cdot \frac{5b}{2\sqrt{16a^2 + 75bc}} \\ &= \lim_{b\to 0} \frac{15c}{2\sqrt{16a^2 + 75bc}} \\ &= \frac{15c}{8a},\end{aligned} \tag{42}$$

$$\begin{aligned}\lim_{b\to 0-0} \frac{\beta}{\lambda} &= \lim_{b\to 0-0} -\frac{8a}{5b} \cdot \frac{5b}{2\sqrt{16a^2 + 75bc}} \\ &= -1,\end{aligned} \tag{43}$$

$$\begin{aligned}\lim_{b\to 0-0} \frac{\beta^2 - 4\alpha}{\lambda^2} &= \lim_{b\to 0-0} \left(\frac{\beta}{\lambda}\right)^2 - 4\frac{\alpha}{\lambda} \cdot \frac{1}{\lambda} \\ &= 1.\end{aligned} \tag{44}$$

We have

$$\begin{aligned}\lim_{b\to 0-0} u_d &= \lim_{b\to 0-0} \left(\frac{4\alpha\lambda}{\lambda^2 e^{-\tau_1\xi} - 2\lambda\beta + (\beta^2 - 4\alpha) e^{\tau_1\xi}}\right)^2 \\ &= \lim_{b\to 0-0} \left(\frac{4\alpha/\lambda}{e^{-\tau_1\xi} - 2(\beta/\lambda) + ((\beta^2 - 4\alpha)/\lambda^2) \cdot e^{\tau_1\xi}}\right)^2 \\ &= u_d^\circ\end{aligned} \tag{45}$$

(see (33)).

Similarly, we have

$$\lim_{b\to 0-0} u_e = u_e^\circ \tag{46}$$

(see (34)).

From (41)–(46), we get result (3) of Proposition 5. □

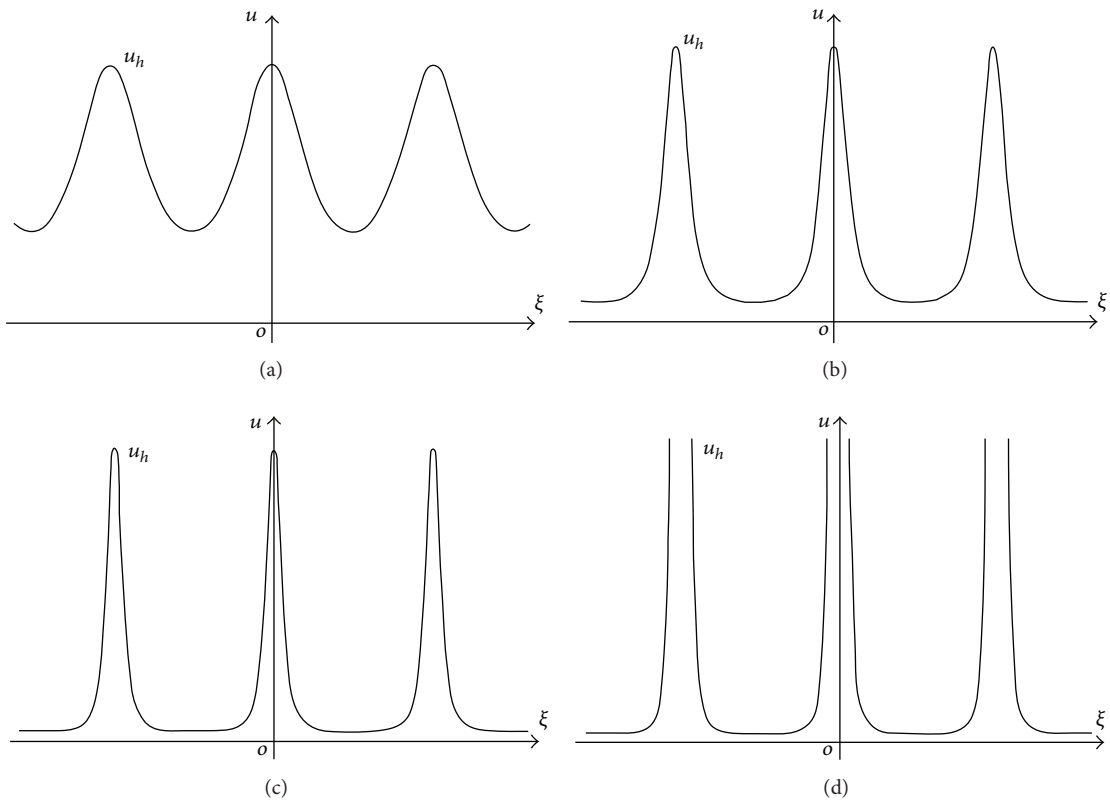

Figure 18: (The periodic blow-up wave is bifurcated from the periodic wave). The varying process for the graph of u_h when $c > 0$, $\delta < 0$, $a > 0$, $\eta > 0$, and $b \to 0-0$, where $c = 1$, $\delta = -1$, $a = 1$, $\eta = 1.57$, and (a) $b = 0-0.2$. (b) $b = 0-0.1$. (c) $b = 0-0.05$. (d) $b = 0-0.01$.

3.2. Bifurcation from Blow-Up Waves

Proposition 6. *For $ab \neq 0$ and $\delta > 0$, (1) has two nonlinear wave solutions as u_d and u_e. These solutions possess the following properties.*

(1) Under one of the following Cases.

Case 1. $\lambda > 0$, $\lambda \neq \sqrt{\beta^2 - 4\alpha}$, and (a, b) belongs to one of the regions A_1, A_3,

Case 2. $\lambda < 0$, $\lambda \neq -\sqrt{\beta^2 - 4\alpha}$, and (a, b) belongs to any one of the regions A_2, A_3, and A_6, $u_d \neq u_e$ and they represent two blow-up waves.

In particular, when $(a, b) \in A_3$ in Case 1 and $b \to -16a^2/75c - 0$, the two blow-up waves become a kink wave and an antikink wave with the expressions (29). *For the varying process, see Figures 9 and 10.*

Similar to the proof of Proposition 5, we get the results of Proposition 6.

3.3. Bifurcation from Valley-Shape Solitary Waves

Proposition 7. *When the parameters satisfy $\delta > 0$ and $(a, b) \in A_3$, (1) has two valley-shape solitary wave solutions $u_f = \varphi(\xi)$ and $u_g = \varphi(\xi)$, respectively, which are hidden in the following equations:*

$$\int_{\varphi_2}^{\varphi} \frac{ds}{\sqrt{(c/\delta)\, s^2 - (8a/15\delta)\, s^{5/2} - (b/3\delta)\, s^3 + h_1}} = \xi \quad (0 < \varphi < \varphi_1), \tag{47}$$

$$\int_{\varphi_2}^{\varphi} \frac{ds}{\sqrt{(c/\delta)\, s^2 - (8a/15\delta)\, s^{5/2} - (b/3\delta)\, s^3 + h_1}} = -\xi \quad (0 < \varphi < \varphi_1). \tag{48}$$

In particular, when $b \to -16a^2/75c - 0$, the two valley-shape solitary waves become a kink wave and an antikink wave with the expressions (29). *For the varying process, see Figures 11 and 12.*

Proof. When $\delta > 0$ and $(a, b) \in A_3$, $(\varphi_1, 0)$ is a saddle point and on its left side there is an orbit Γ_3 connecting with it (see Figure 13).

In (8), letting $h_1 = H(\varphi_1, 0)$, it follows that

$$\Gamma_3 : y^2 = \frac{c}{\delta}\varphi^2 - \frac{8a}{15\delta}\varphi^{5/2} - \frac{b}{3\delta}\varphi^3 + h_1 \quad (0 < \varphi < \varphi_1). \tag{49}$$

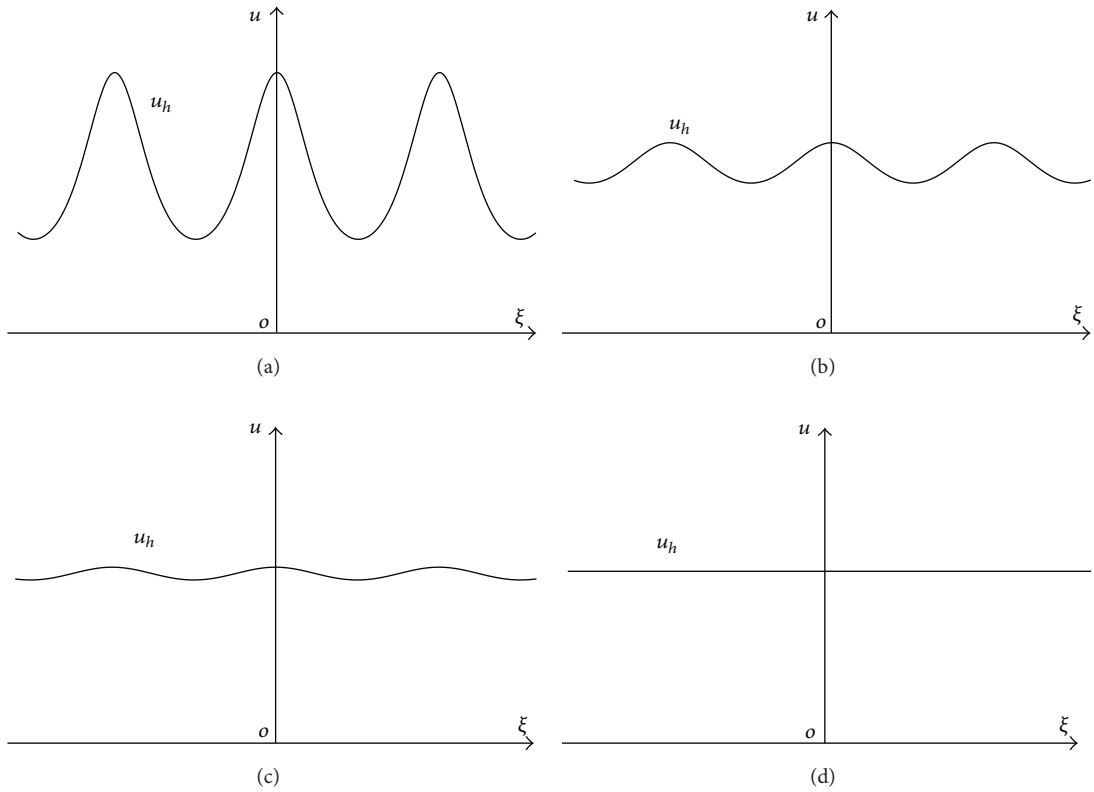

Figure 19: (The periodic wave become the trivial wave). The varying process for the graph of u_h when $c > 0$, $\delta < 0$, $a > 0$, $\eta < 0$, and $b \to -16a^2/75c + 0$, where $c = 1$, $\delta = -1$, $a = 1$, $\eta = -4.7$, and (a) $b = -16a^2/75c + 10^{-2}$. (b) $b = -16a^2/75c + 10^{-3}$. (c) $b = -16a^2/75c + 10^{-4}$. (d) $b = -16a^2/75c + 10^{-7}$.

Substituting (49) into (7) and integrating it along the orbit Γ_3, we get (47) and (48).

Letting $b \to -16a^2/75c - 0$, it follows that

$$\begin{aligned}\lim_{b\to -16a^2/75c-0} h_1 &= \lim_{b\to -16a^2/75c-0} H(\varphi_1, 0)\\ &= \lim_{b\to -16a^2/75c-0} -\frac{c}{\delta}\varphi_1^2 + \frac{8a}{15\delta}\varphi_1^{5/2} + \frac{b}{3\delta}\varphi_1^3\\ &= 0.\end{aligned} \tag{50}$$

When $h_1 \to 0$, completing the integrals in (47) and (48), we get the kink wave solution and the antikink wave solution as (29).

Hereto, we have completed the proof for the Proposition 7. □

3.4. Bifurcation from Kink-Like Waves

Proposition 8. *When the parameters satisfy $\delta > 0$, $(a, b) \in A_2$, and $b \to -16a^2/75c + 0$, the kink-like wave and the antikink-like wave, respectively, become a kink wave and an anti-kink wave with the expressions* (29).

For the varying process, see Figures 14 and 15.

Proof. Letting $b \to -16a^2/75c + 0$, it follows that $h_1 \to 0$ (see (50)) and

$$\begin{aligned}&\lim_{b\to -16a^2/75c+0} \xi_1^0\\ &= \int_0^{\varphi_1/2} \frac{ds}{\sqrt{(c/\delta)s^2 - (8a/15\delta)s^{5/2} + (16a^2/225c\delta)s^3}}\\ &= \lim_{\nu\to 0}\int_\nu^{\varphi_1/2} \frac{ds}{\sqrt{(c/\delta)s^2 - (8a/15\delta)s^{5/2} + (16a^2/225c\delta)s^3}}\\ &= \infty.\end{aligned} \tag{51}$$

When $h_1 \to 0$, and $\xi_1^0 \to \infty$, completing the integrals in (17), we get the kink wave solution and the antikink wave solution as (29).

Hereto, we have completed the proof for the Proposition 8. □

3.5. Bifurcation from Compacton-Like Waves

Proposition 9. *When the parameters satisfy $\delta > 0$, $(a,b) \in A_2$, and $b \to -16a^2/75c + 0$, the two compacton-like waves become a kink wave and an anti-kink wave with the expressions* (29).

For the varying process, see Figures 16 and 17.

Proof. Letting $b \to -16a^2/75c + 0$, it follows that

$$\begin{aligned}\lim_{b\to -16a^2/75c+0} h_{\varphi_k} &= \lim_{b\to -16a^2/75c+0} H(\varphi_k, 0)\\ &= \lim_{b\to -16a^2/75c+0} -\frac{c}{\delta}\varphi_k^2 + \frac{8a}{15\delta}\varphi_k^{5/2} + \frac{b}{3\delta}\varphi_k^3\\ &= 0,\end{aligned} \tag{52}$$

$$\begin{aligned}&\lim_{b\to -16a^2/75c+0} \xi_3^0\\ &= \int_0^{\varphi_k/2} \frac{ds}{\sqrt{(c/\delta)s^2 - (8a/15\delta)s^{5/2} + (16a^2/225c\delta)s^3}}\\ &= \lim_{\nu\to 0}\int_\nu^{\varphi_k} \frac{ds}{\sqrt{(c/\delta)s^2 - (8a/15\delta)s^{5/2} + (16a^2/225c\delta)s^3}}\\ &= \infty,\end{aligned} \tag{53}$$

$$\begin{aligned}&\lim_{b\to -16a^2/75c+0} \xi_4^0\\ &= \lim_{b\to -16a^2/75c+0}\left(2\int_{\varphi_k/2}^{\varphi_k} (ds)\left((c/\delta)s^2 - (8a/15\delta)s^{5/2}\right.\right.\\ &\qquad \left.\left. - (b/3\delta)s^3 + h_{\varphi_k}\right)^{-1/2}\right)\\ &\qquad + \xi_3^0\Bigg) = \infty.\end{aligned} \tag{54}$$

When $h_{\varphi_k} \to 0$, $\xi_3^0 \to \infty$, and $\xi_4^0 \to \infty$, completing the integrals in (21), we get the kink wave solution and the antikink wave solution as (29).

Hereto, we have completed the proof for the Proposition 9. □

4. Bifurcation of Smooth Periodic Wave

Proposition 10. *For $ab \neq 0$ and $\delta < 0$,* (1) *has a nonlinear wave solution*

$$u_h = \left(\frac{-2\alpha}{\sqrt{\beta^2 - 4\alpha}\sin(\tau_2\xi + \eta) + \beta}\right)^2, \tag{55}$$

where

$$\tau_2 = \frac{1}{2}\sqrt{-\frac{c}{\delta}}, \tag{56}$$

and η is an arbitrary real number. The solution possesses the following properties.

(1) *if (a,b) belongs to any one of the regions A_1, A_6, then u_h represents periodic blow-up wave solution,*

(2) *if (a,b) belongs to A_2, then u_h represents periodic wave solution.*

In particular, when $b \to 0-0$, the periodic wave becomes a periodic blow-up wave. For the varying process, see Figure 18. When $b \to -16a^2/75c + 0$, the periodic wave tends to a trivial wave $u = 225c^2/16a^2$. For the varying process, see Figure 19.

Proof. Completing the integral in (38), we get u_h as (55). $\eta = \eta(\nu)$ is an arbitrary real number.

When $(a,b) \in A_2$, in (38) letting $\nu = q$ (see (28)), we have

$$\eta = \arcsin\frac{-\beta q - 2\alpha}{q\sqrt{\beta^2 - 4\alpha}}. \tag{57}$$

Letting $b \to 0-0$, then

$$\begin{aligned}\lim_{b\to 0-0}\sqrt{\frac{\beta^2 - 4\alpha}{\beta^2}} &= \lim_{b\to 0-0}\sqrt{\frac{75bc}{16a^2} + 1} = 1,\\ \lim_{b\to 0-0}\eta &= \lim_{b\to 0-0}\arcsin\frac{-\beta q - 2\alpha}{q\sqrt{\beta^2 - 4\alpha}}\\ &= \lim_{b\to 0-0}\arcsin\left(\frac{1}{\sqrt{(\beta^2 - 4\alpha)/\beta^2}}\right.\\ &\qquad \left. + \frac{2}{q\sqrt{(\beta^2 - 4\alpha)/\alpha^2}}\right)\\ &= \arcsin 1\\ &= \frac{\pi}{2}.\end{aligned} \tag{58}$$

We have

$$\lim_{b\to 0-0} u_h = \lim_{b\to 0-0}\left(\frac{-2\alpha}{\sqrt{\beta^2-4\alpha}\sin(\tau_2\xi+\eta)+\beta}\right)^2$$
$$= \lim_{b\to 0-0}\left(\frac{2\alpha/\beta}{\sqrt{(\beta^2-4\alpha)/\beta^2}\sin(\tau_2\xi+\eta)-1}\right)^2$$
$$= \frac{225c^2}{16a^2[\cos(\tau_2\xi)-1]^2}. \tag{59}$$

Obviously, u_h will blow up when $\xi = 2k\pi/\tau_2$ $(k \in z)$.

Hereto, we have completed the proofs for all propositions. □

5. Conclusion

In this paper, we have studied the bifurcation behavior of S-KdV equation. Two new types of nonlinear waves called kink-like waves and compacton-like waves have been displayed in Propositions 1–3. Furthermore, two kinds of new bifurcation phenomena have been revealed. The first phenomenon is that the kink waves can be bifurcated from five types of nonlinear waves which have been stated in Propositions 5–9. The second phenomenon is that the periodic blow-up wave can be bifurcated from the periodic wave which has been explained in Proposition 10. At the same time, we have got three new explicit expressions for traveling waves which were given in (25) and (55). Two previous results are our some special cases (see (30) and (32)).

Acknowledgments

This work is supported by the National Natural Science Foundation of China (no. 11171115) and the Science and Technology Foundation of Guizhou (no. LKS[2012]14).

References

[1] S. G. Tagare and A. N. Chakraborty, "Solution of a generalised Korteweg-de Vries equation," *Physics of Fluids*, vol. 17, no. 6, article 1331, 2 pages, 1974.

[2] G. C. Das, S. G. Tagare, and J. Sarma, "Quasi-potential analysis for ion-acoustic solitary wave and double layers in plasmas," *Planetary and Space Science*, vol. 46, no. 4, pp. 417–424, 1998.

[3] J. Lee and R. Sakthivel, "Exact travelling wave solutions of the Schamel-Korteweg-de Vries equation," *Reports on Mathematical Physics*, vol. 68, no. 2, pp. 153–161, 2011.

[4] H. Schamel, "A modified Korteweg-de Vries equation for ion acoustic waves due to resonant electrons," *Plasma Physics*, vol. 9, no. 3, pp. 377–387, 1973.

[5] G. C. Das and K. M. Sen, "Various turbulences in ion-acoustic solitary waves in plasmas," *Planetary and Space Science*, vol. 42, no. 1, pp. 41–46, 1994.

[6] R. M. Miura, "The Korteweg-de Vries equation: a survey of results," *SIAM Review*, vol. 18, no. 3, pp. 412–459, 1976.

[7] R. K. Dodd, J. C. Eilbeck, J. D. Gibbon, and H. C. Morris, *Solitons and Nonlinear Wave Equations*, Academic Press, London, UK, 1982.

[8] X. B. Wu, W. G. Rui, and X. C. Hong, "A generalized KdV equation of neglecting the highest-order infinitesimal term and its exact traveling wave solutions," *Abstract and Applied Analysis*, vol. 2013, Article ID 656297, 15 pages, 2013.

[9] P. Rosenau and J. M. Hyman, "Compactons: solitons with finite wavelength," *Physical Review Letters*, vol. 70, no. 5, pp. 564–567, 1993.

[10] P. Rosenau, "Nonlinear dispersion and compact structures," *Physical Review Letters*, vol. 73, no. 13, pp. 1737–1741, 1994.

[11] P. Rosenau, "On solitons, compactons, and Lagrange maps," *Physics Letters A*, vol. 211, no. 5, pp. 265–275, 1996.

[12] P. Rosenau, "Compact and noncompact dispersive patterns," *Physics Letters A*, vol. 275, no. 3, pp. 193–203, 2000.

[13] A. M. Wazwaz, "New solitary-wave special solutions with compact support for the nonlinear dispersive $K(m,n)$ equations," *Chaos, Solitons and Fractals*, vol. 13, no. 2, pp. 321–330, 2002.

[14] A. M. Wazwaz, "Compactons dispersive structures for variants of the $K(n,n)$ and the KP equations," *Chaos, Solitons and Fractals*, vol. 13, no. 5, pp. 1053–1062, 2002.

[15] A.-M. Wazwaz, "Solutions of compact and noncompact structures for nonlinear Klein-Gordon-type equation," *Applied Mathematics and Computation*, vol. 134, no. 2-3, pp. 487–500, 2003.

[16] A. M. Wazwaz and T. Taha, "Compact and noncompact structures in a class of nonlinearly dispersive equations," *Mathematics and Computers in Simulation*, vol. 62, no. 1-2, pp. 171–189, 2003.

[17] A. M. Wazwaz, "An analytic study of compactons structures in a class of nonlinear dispersive equations," *Mathematics and Computers in Simulation*, vol. 63, no. 1, pp. 35–44, 2003.

[18] A. M. Wazwaz, "Two reliable methods for solving variants of the KdV equation with compact and noncompact structures," *Chaos, Solitons and Fractals*, vol. 28, no. 2, pp. 454–462, 2006.

[19] Z. R. Liu, Q. M. Lin, and Q. X. Li, "Integral approach to compacton solutions of Boussinesq-like $B(m,n)$ equation with fully nonlinear dispersion," *Chaos, Solitons and Fractals*, vol. 19, no. 5, pp. 1071–1081, 2004.

[20] Z. R. Liu, Q. X. Li, and Q. M. Lin, "New bounded traveling waves of Camassa-Holm equation," *International Journal of Bifurcation and Chaos in Applied Sciences and Engineering*, vol. 14, no. 10, pp. 3541–3556, 2004.

[21] Z. S. Wen, "Extension on bifurcations of traveling wave solutions for a two-component Fornberg-Whitham equation," *Abstract and Applied Analysis*, vol. 2012, Article ID 704931, 15 pages, 2012.

[22] M. Song, "Application of bifurcation method to the generalized Zakharov equations," *Abstract and Applied Analysis*, vol. 2012, Article ID 308326, 8 pages, 2012.

[23] F. Faraci and A. Iannizzotto, "Bifurcation for second-order Hamiltonian systems with periodic boundary conditions," *Abstract and Applied Analysis*, vol. 2008, Article ID 756934, 13 pages, 2008.

[24] Z. R. Liu and Y. Long, "Compacton-like wave and kink-like wave of GCH equation," *Nonlinear Analysis: Real World Applications*, vol. 8, no. 1, pp. 136–155, 2007.

[25] S. L. Xie and L. Wang, "Compacton and generalized kink wave solutions of the CH-DP equation," *Applied Mathematics and Computation*, vol. 215, no. 11, pp. 4028–4039, 2010.

[26] P. J. Olver and P. Rosenau, "Tri-Hamiltonian duality between solitons and solitary-wave solutions having compact support," *Physical Review E*, vol. 53, no. 2, pp. 1900–1906, 1996.

[27] M. S. Ismail and T. R. Taha, "A numerical study of compactons," *Mathematics and Computers in Simulation*, vol. 47, no. 6, pp. 519–530, 1998.

[28] A. Ludu and J. P. Draayer, "Patterns on liquid surfaces: cnoidal waves, compactons and scaling," *Physica D*, vol. 123, no. 1–4, pp. 82–91, 1998.

[29] J. H. He and X. H. Wu, "Construction of solitary solution and compacton-like solution by variational iteration method," *Chaos, Solitons & Fractals*, vol. 29, no. 1, pp. 108–113, 2006.

[30] S. Kuru, "Compactons and kink-like solutions of BBM-like equations by means of factorization," *Chaos, Solitons & Fractals*, vol. 42, no. 1, pp. 626–633, 2009.

[31] G. Mussardo, "Neutral bound states in kink-like theories," *Nuclear Physics B*, vol. 779, no. 3, pp. 101–154, 2007.

[32] R. S. Han, J. L. Yang, L. Huibin, and W. Kelin, "Exact travelling kink-like wave solutions to some nonlinear equations," *Physics Letters A*, vol. 236, no. 4, pp. 319–321, 1997.

[33] S. Dusuel, P. Michaux, and M. Remoissenet, "From kinks to compactonlike kinks," *Physical Review E*, vol. 57, no. 2, pp. 2320–2326, 1998.